Meas. Sci. Technol. **22** (2011) 094025 (6pp) doi:10.1088/0957-0233/22/9/094025

High-accuracy Fabry–Perot displacement interferometry using fiber lasers

Mathieu Durand, John Lawall and Yicheng Wang

National Institute of Standards and Technology, Gaithersburg, MD 20899, USA

E-mail: john.lawall@nist.gov

Received 9 January 2011, in final form 17 March 2011
Published 8 August 2011
Online at stacks.iop.org/MST/22/094025

Abstract
We describe ongoing work in a Fabry–Perot interferometry system designed to measure displacements over a range of 50 mm with sub-pm uncertainty. The apparatus involves probing two nearby modes of the Fabry–Perot cavity with narrow-linewidth fiber telecom lasers and measuring both the mode spacing and the absolute mode frequencies relative to a third, frequency-stabilized, fiber laser. We explore the improvement in resolution obtained as the frequency separation between the two modes is increased and employ an internal consistency requirement to infer the magnitude of residual systematic errors. The measurement uncertainty is sufficiently small that we are easily able to see the Gouy phase shift as the cavity length is changed over several millimeters.

Keywords: Fabry–Perot, interferometry, displacement metrology, Gouy phase

(Some figures in this article are in colour only in the electronic version)

1. Introduction

Accurate measurements of displacement are essential to many applications in manufacturing and scientific research [1]. Various types of laser interferometry are commonly used for such measurements [2]. While 'two-beam' interferometry, characterized by a sinuosoidal optical fringe [3–5], is the most common, Fabry–Perot interferometry [6–9] has been noted to possess a number of distinct advantages for the most demanding tasks [10]. Recent work [11, 12] is exploring the benefits that may be derived from using advanced frequency-comb techniques. In 2005, one of us (JL) probed two adjacent modes of a Fabry–Perot cavity with light from a helium–neon laser at 633 nm [10]. In that work, the measurement of changes in mode spacing alone was sufficient to determine cavity length changes with an uncertainty of $\delta L = 21$ nm, and by employing an iodine-stabilized laser as an optical reference, displacements were measured over a distance of 25 mm with an uncertainty below 10 pm.

In this work, we are revisiting this approach, using fiber lasers at a wavelength of 1560 nm. This work is underway in order to make a new 'calculable capacitor' [13], a realization of the SI (International System of Units) farad in terms of an accurately measured mechanical displacement. The displacement is to be made over a range of 50 mm, centered around a length of 85 mm. The fiber lasers are tunable over a much broader range than helium–neon lasers, and fine tuning by means of a piezoelectric transducer is sufficiently rapid that the use of acousto-optic modulators, as done in [10], is not required. Moreover, the use of telecom fiber components makes the system vastly simpler and more robust. Most importantly, the performance of the present system promises to be considerably better than that obtained formerly with the helium–neon-based system.

In this paper, we explore two aspects of the new implementation which are of particular importance for high-accuracy measurement. First, due to the large tuning range of the fiber lasers, we are able to span a much larger mode spacing than was done in the earlier work, yielding improved resolution and accuracy. Second, displacement measurements may be made either by interpretation of changes in the Fabry–Perot cavity mode spacing or by measurement of changes in the absolute frequency of cavity modes; the associated redundancy provides a powerful check for systematic errors. In this way, we have established that the level of systematic errors present in the current system should allow for displacement measurements with an accuracy of 25 fm over distances up to 4 μm (assuming a perfect optical reference). In subsequent work, we will extend this analysis to find the corresponding limitation over the full 50 mm measurement range. For

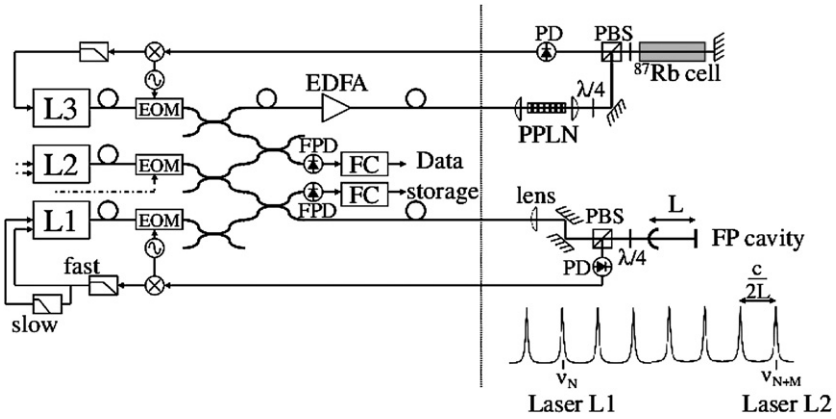

Figure 1. Experimental apparatus. EOM: electro-optic modulator; EDFA: erbium-doped fiber amplifier; FPD: fast photodiode; PPLN: periodically poled lithium niobate; PBS: polarizing beam splitter; PD: photodiode; FP: Fabry–Perot cavity; FC: frequency counter. Light from fibers lasers L1 and L2 is combined, collimated and locked to two nearby modes ν_N and ν_{N+M} of a Fabry–Perot cavity. Light from a third fiber laser L3 is frequency-doubled and locked to a Rb cell to provide an optical frequency reference. The beats between lasers L1 and L2 and between L2 and L3 are observed with fast (20 GHz) detectors and counted.

the moment, we merely show that the uncertainty is small enough to allow us to observe the influence of the Gouy phase shift in the measurement of a displacement of several millimeters.

2. Principles of Fabry–Perot displacement metrology

2.1. Review of fundamentals

We start by briefly summarizing Fabry–Perot displacement metrology using tunable lasers [10]. The Fabry–Perot cavity is assumed to be formed of one flat mirror and one curved mirror with a radius of curvature R, separated by a distance L (figure 1). We consider only the case where the cavity finesse is high. Laser light is resonant with the cavity when its frequency matches one of the cavity resonance frequencies ν_N given approximately by

$$\nu_N = \frac{c}{2L}N, \tag{1}$$

where c is the speed of light in vacuum and N is an integer. (It is implicitly assumed that the cavity is operated in vacuum; if not, the length L would need to be replaced with nL, where n is the index of refraction of the gas in the cavity, and if n varies with frequency, then equation (1) requires further modification.) Thus, if feedback is employed to lock a tunable laser to a cavity resonance, changes δL in the cavity length manifest themselves as changes $\delta\nu_N$ in the cavity resonance frequency. A more accurate formulation [10], properly accounting for diffraction and phase shifts upon reflection, is

$$\nu_N = \frac{c}{2L}\frac{1}{1+\frac{\alpha}{2\pi}\frac{c}{2L}}\left[N+\frac{1}{2\pi}(2\Phi(L)-\phi_{\text{refl}})\right], \tag{2}$$

where $\Phi(L) = \sin^{-1}\sqrt{L/R}$ is the Gouy (or Fresnel) phase shift associated with diffraction of a Gaussian beam, and ϕ_{refl} and α are (unknown) constants associated with reflective phase shifts at the cavity mirrors. In any case, by comparing a change in the resonance frequency $\delta\nu_N$ to an optical reference, δL can be determined. The utility of this approach to displacement determination is limited, however, by the range over which the tunable laser can follow a change in mode frequency [6, 10].

This difficulty can be largely overcome by probing two modes of the cavity rather than only one, as the absolute cavity length L determines the mode spacing (free spectral range). Using the complete expression (2) for the mode frequencies, the difference $\Delta\nu_{N+M,N}$ between the frequencies of modes N and $N+M$ is

$$\Delta\nu_{N+M,N} \equiv \Delta\nu_M = \frac{c}{2L}\frac{M}{1+\frac{\alpha}{2\pi}\frac{c}{2L}}, \tag{3}$$

where the more compact notation $\Delta\nu_M$ is used since the expression for $\Delta\nu_{N+M,N}$ is independent of N. Equation (3) can be solved for the cavity length L in terms of the mode spacing, and one obtains for the measured length

$$L_{\text{meas}} = \frac{c}{2}\left[\frac{M}{\Delta\nu_M}-\frac{\alpha}{2\pi}\right]. \tag{4}$$

This approach to determining the cavity length has been dubbed the 'rf method', as the measurement of $\Delta\nu_M$ is done by means of radio-frequency (rf) or microwave electronics, with no optical frequency reference. In this formulation, it is not necessary to track a particular mode N. Whatever the cavity length, one simply locks the two lasers to any two nearby modes. The (small) constant term $\frac{\alpha}{2\pi}$ reflects the fact that the optical field penetrates the dielectric mirror on a length scale set by the wavelength of the light. This term drops out in the measurement of a displacement.

2.2. Relation of resolution to mode spacing

In the previous work [10], the limited tuning range of the acousto-optic modulators allowed only for a measurement of adjacent modes ($M = 1$). With the advent of fiber lasers that can be swept over more than 10 GHz, we are able to span a much larger mode spacing. It is straightforward to show that this can yield a correspondingly better resolution. Differentiating equation (4), one finds

$$\delta L_{\text{meas}} = L_{\text{meas}}\frac{\delta(\Delta\nu_M)}{\Delta\nu_M}. \tag{5}$$

Fluctuations in the measured value of $\Delta\nu_M$ are determined partly by the fluctuations of the laser frequency about the mean–mode frequencies ν_N and ν_{N+M}, and partly by actual fluctuations in the cavity length L. For simplicity, we assume that these fluctuations are uncorrelated, and the laser-frequency fluctuations are governed by electronic noise in the servo. Denoting the laser-frequency fluctuations by $\delta\nu_{\text{servo}}$, one has

$$\delta(\Delta\nu_M) = \sqrt{2\delta\nu_{\text{servo}}^2 + \frac{\delta L^2}{L^2}\Delta\nu_M^2}. \tag{6}$$

Substitution of $\delta(\Delta\nu_M)$ into equation (5) yields

$$\delta L_{\text{meas}} = \sqrt{2L_{\text{meas}}^2\frac{\delta\nu_{\text{servo}}^2}{\Delta\nu_M^2} + \delta L^2}. \tag{7}$$

Thus, in the case of a perfectly stable cavity ($\delta L = 0$), the resolution in the length measurement is expected to scale inversely with the mode spacing $\Delta\nu_M$ probed. In this work, we are limited by the photodetector bandwidth to a mode spacing of 20 GHz.

3. Experiment

3.1. Apparatus

The experimental apparatus, shown in figure 1, has been described previously [14]. Briefly, light from fiber lasers L1 and L2 is combined and collimated, and then mode-matched into a Fabry–Perot cavity with a finesse of $F \approx 20\,000$ whose length can be varied over 6 μm by means of a piezoelectric actuator. The nominal cavity length is set by an aluminum spacer and the cavity is presently operated in air. The lasers are independently locked to nearby modes of the cavity and the beat frequency between the lasers is recorded by means of a photodetector (20 GHz bandwidth) and microwave counter. An optical reference is formed by frequency-doubling a third fiber laser L3 and locking the doubled light (780 nm) by means of saturated absorption to a rubidium transition. The beat frequency between lasers L2 and L3 is also measured and counted.

3.2. Mode spacing

In order to assess the dependence of the length resolution on the number of modes spanned, we locked lasers L1 and L2 to modes N and $N + M$ for M varying from 1 to 10, and recorded the beat frequency as a function of time. Figure 2(*a*) shows the fractional mode spacing $\delta(\Delta\nu_M)/\langle\Delta\nu_M\rangle$, where the angle brackets indicate a time average, over a period of 60 s for $M = 1$ ($\langle\Delta\nu_M\rangle \approx 1.91$ GHz) and $M = 10$ ($\langle\Delta\nu_M\rangle \approx 19.1$ GHz). It is clear that the measurement for $M = 10$ is substantially less noisy, as expected, at high frequencies, but at low frequencies the mean-square fractional frequency change is similar. This arises from the fact that the aluminum cavity under test is not stable. More quantitatively, figure 2(*b*) shows the Allan deviation of the fractional frequency fluctuations for the same separations $M = 1$ and $M = 10$. For the smallest averaging times, the fractional fluctuations are about a factor of four smaller for the case of $M = 10$ than they are for $M = 1$, and at larger times, the fluctuations in the cavity length start to dominate and the distinction between $M = 1$ and $M = 10$ becomes less pronounced.

We now return to the issue of the length fluctuations inferred as a function of the number of modes, M, spanned. Figure 3 shows a log–log plot of the length fluctuations found for M taking all integral values from 1 to 10. Clearly, the length fluctuations diminish as M increases, corresponding to better measurement resolution. The rate of improvement, however, also diminishes as M increases. For a perfectly stable cavity, equation (7) implies

$$\delta L_{\text{meas}} = \sqrt{2}L_{\text{meas}}\frac{\delta\nu_{\text{servo}}}{\Delta\nu_M}. \tag{8}$$

The dotted line in figure 3 has a slope of -1, showing that the behavior embodied in equation (8) is only asymptotically approached for the smallest values of M. Fluctuations in the (optical) cavity length, due both to thermal expansion and contraction of the aluminum spacer and fluctuations in the index of refraction of air, are the cause. Nevertheless, we are able to resolve length variations at the level of 2×10^{-11} m Hz$^{-1/2}$ using only rf techniques to monitor changes in the optical mode spacing. Ultimately, we plan to work in vacuum and lock the cavity length to the interferometer output, rather than the other way around as we do here.

3.3. Optical reference

Until now, all measurements discussed have been based on the difference in mode frequencies, rather than absolute mode frequencies. We now return to the idea of measuring displacements relative to an optical reference, as embodied in equation (1) and, more accurately, equation (2). Comparing equation (2) to equation (3) at the heart of the 'rf method', it is apparent that the resolution of a measurement employing an optical reference can be expected to be higher by a factor of approximately N/M. In our case (cavity with a nominal length $L \approx 100$ mm and wavelength $\lambda = 1560$ nm), and with $\Delta\nu_M$ limited to 20 GHz, the expected enhancement in resolution provided by the optical reference is approximately 10^4. While this figure assumes a perfect optical reference, in practice the enhancement can still be expected to be substantial. This matter will be discussed more thoroughly below.

Figure 4 shows a comparison of three cavity length ($L \approx 80$ mm) measurements, in which the rf method is used in the domain where the performance is limited by servo noise (dashed line) , the rf method is used with $M = 10$, and cavity length fluctuations dominate (dotted line), and the optical method (solid line). The measurements using the optical method and the rf method with $M = 10$ were made simultaneously. While the reduction in noise achieved with the rf method by going to $M = 10$ is evident, the optical method appears to give little improvement over the rf measurement with $M = 10$. This is a consequence of the fact that we are not working in vacuum and the fluctuations observed are true fluctuations in the optical path length. This is actually a strong testament to the power of the rf method.

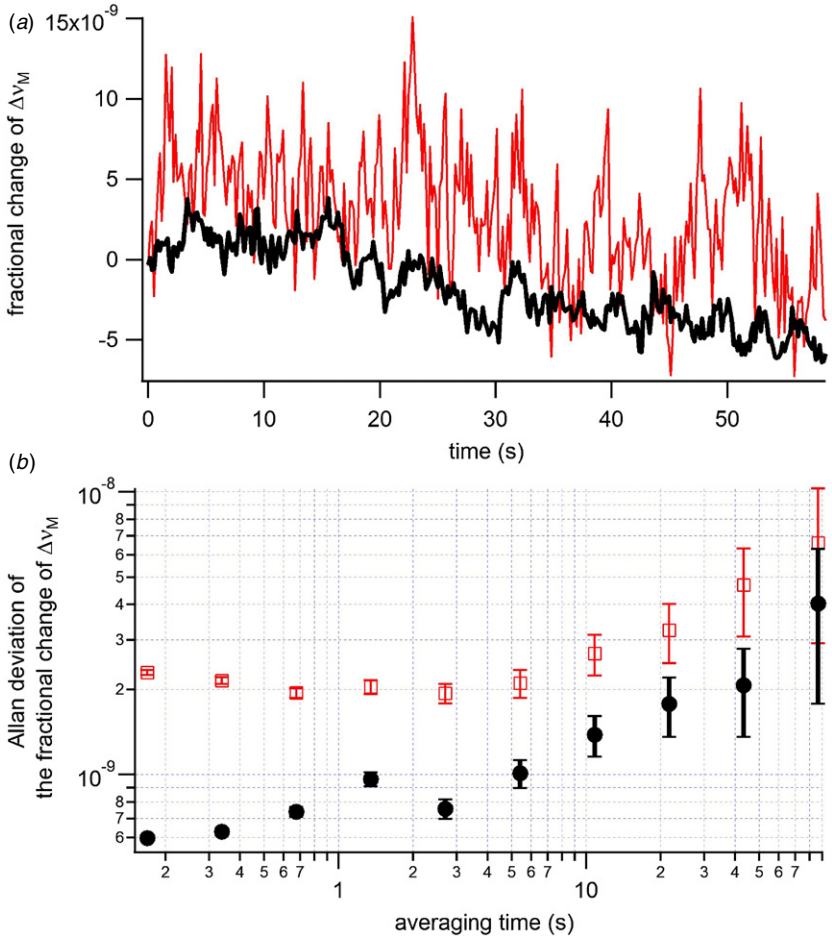

Figure 2. (*a*) Fluctuations in the mode spacing $\Delta\nu_M$ normalized to the mean value of $\Delta\nu_M$, for $M = 1$ (thin line) and $M = 10$ (bold line). Interrogating a larger mode spacing reduces the influence of noise imposed by the servo loops, but the slow variations are similar since they are due to cavity length drifts. (*b*) Corresponding Allan deviation with square markers for $M = 1$ and circular markers for $M = 10$. Error bars correspond to the Allan deviation divided by the square root of the number of samples used in its computation. The improvement due to spanning a large number of modes is particularly evident for small integration times. For larger times, the improvement is masked by variations in the cavity length.

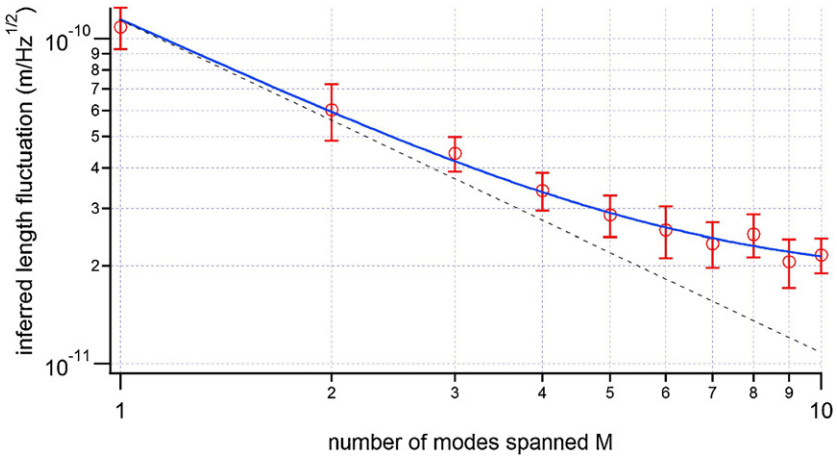

Figure 3. Length fluctuations δL inferred as a function of the number of modes M spanned. The experimental data points (markers) are fitted using equation (7) (line). The error bars reflect the standard deviation of 20 successive measurements, each of 16 s duration acquired at a rate of 6 Hz. Increasing M improves the resolution, but the rate of improvement observed diminishes as M increases, owing to fluctuations in the optical cavity length. The dotted line has a slope of -1, corresponding to the ideal case of resolution inversely proportional to M.

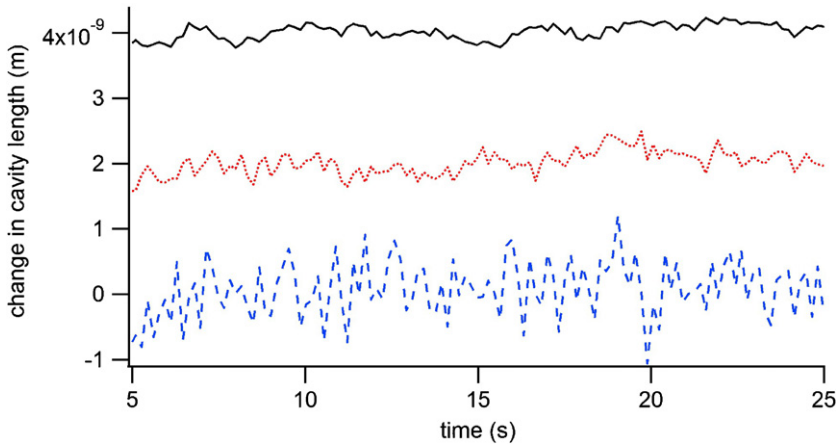

Figure 4. Time variation of cavity length measurements made with three different methods. Dashed line: rf method dominated by servo noise; dotted line: rf method with $M = 10$, where length fluctuations dominate servo noise; solid line: optical method. All traces are fluctuations about the mean measured cavity length, and are offset from one another by 2 nm for clarity.

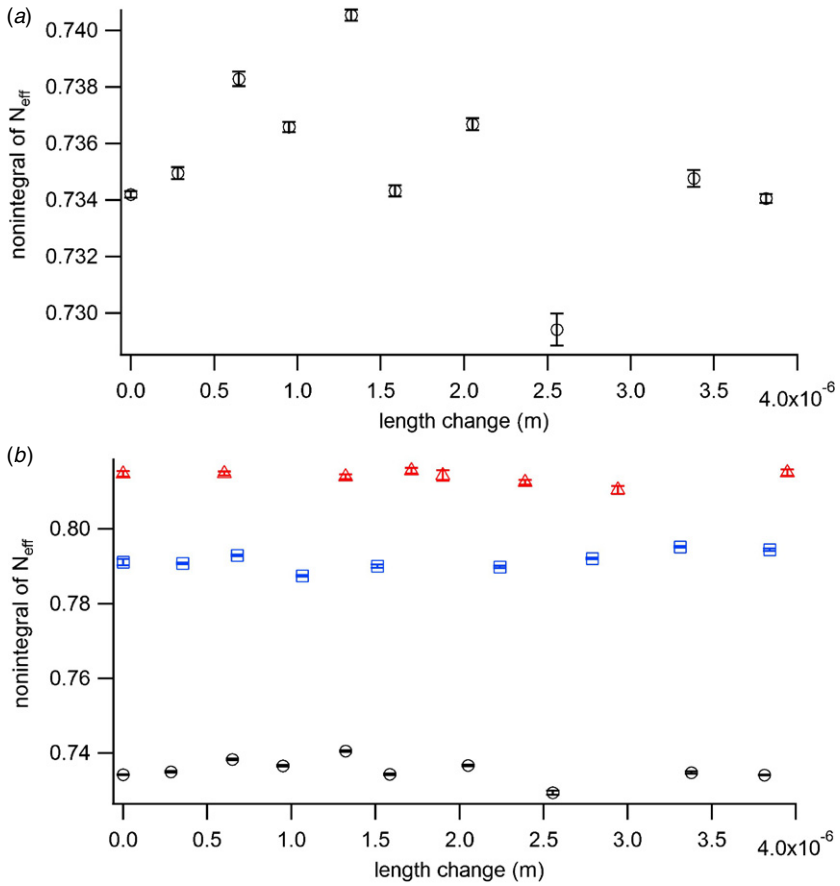

Figure 5. (*a*) Nonintegral parts of the 'effective order number' N_{eff} defined in equation (9). The standard deviation is $\sigma = 3 \times 10^{-3}$ and the integral parts of N_{eff} vary from 86 236 to 86 242. (*b*) Similar data for nominal cavity lengths of 68 mm (circles), 78 mm (squares) and 82 mm (triangles). The different mean values are due to the Gouy phase shift.

3.4. Internal consistency verification using optical reference

By working in vacuum it can be expected that the resolution obtained with the optical method can be used to advantage. This enhanced resolution only translates to accuracy, however, in the absence of parasitic Fabry–Perot cavities and other sources of systematic error that can shift the laser lock point away from the actual mode frequencies ν_N and ν_{N+M}. Remarkably, the measurement redundancy present in measuring displacements via the optical and rf methods provides a powerful check for the presence of such systematic errors [10]. Dividing equation (2) by equation (3), one obtains

$$\frac{\nu_N}{\Delta\nu} \equiv N_{\text{eff}} = N + \frac{1}{2\pi}(2\Phi(L) - \phi_{\text{refl}}), \tag{9}$$

where

$$\Delta\nu \equiv \frac{\Delta\nu_M}{M}$$

is the free spectral range. The quantity denoted by $N_{\rm eff}$ is the ratio of a measurement made with the optical reference, ν_N, to a rf measurement $\Delta\nu$ of the free spectral range. Equation (9) states that the nonintegral part of this ratio must be equal to a constant plus a term arising from the Gouy phase shift.

Figure 5(*a*) shows the nonintegral parts of $N_{\rm eff}$ arising from a series of independent measurements made with a cavity of nominal length $L = 67$ mm over a distance of 4 μm, in which the integral part of $N_{\rm eff}$ varied from 86 236 to 86 242. Over this range the Gouy phase shift changes are completely negligible. The error bars are purely statistical, and correspond to the standard deviation of 180 measurements performed during a time of 30 s for each cavity length. The fact that the fluctuations between points exceed the statistical uncertainties confirms the presence of uncontrolled systematic errors shifting the measurement lock points. From the standard deviation $\sigma = 3 \times 10^{-3}$ in $N_{\rm eff}$ we can infer an absolute uncertainty (standard deviation) of 78 Hz on the free spectral range measurement. The corresponding relative length uncertainty for the rf method is 3.5×10^{-8}, or 2.3 nm for this cavity length. Assuming the lock points of lasers L1 and L2 to be uncorrelated, we infer uncontrolled random frequency offsets with a standard deviation of 55 Hz in the individual lock points $\nu_{\rm servo}$. The corresponding length uncertainty for the optical method, from equation (1), is 18 fm. This level of length uncertainty is of course only realized if the optical reference has an uncertainty well below 55 Hz; if it does not, then the optical reference, rather than uncontrolled perturbations of the frequency lock point, will limit the measurement uncertainty. We have recently beat laser L3, locked to rubidium, against a frequency comb [15], and found an Allan deviation of 1 kHz after 3 s of averaging time. The corresponding contribution to a cavity length measurement is $\delta L = L\,{\rm d}\nu/\nu = 335$ fm. Figure 5(*b*) shows the result of similar measurements for three macroscopically different cavity lengths obtained by the use of different aluminum spacers. The length fluctuations are of similar magnitude, but the measurements are slightly offset from one another. This offset is a manifestation of the Gouy phase shift. A quantitative evaluation will appear in a future paper. We emphasize that the accuracy in a measurement of the free spectral range is nearly two orders of magnitude better than that required to unambiguously recover the integer part of $N_{\rm eff}$.

4. Conclusion and outlook

We have described ongoing research in the development of a Fabry–Perot interferometry system using fiber lasers at 1560 nm to be used in a new calculable capacitor. Two aspects of this work have been highlighted. First, changes in the cavity length can be measured by purely rf means by monitoring the spacing between nearby cavity modes. We have demonstrated that the resolution can be increased by spanning a greater number of modes. In our case, we are limited to a span of approximately ten modes due to the 20 GHz bandwidth of the photodetector we use to monitor the beat frequency. We demonstrate a length resolution of 2×10^{-11} m Hz$^{-1/2}$, that we believe to be limited essentially by the fluctuations in the index of refraction of air. By use of a frequency comb [15], this approach could be extended to a mode spacing of tens of possibly hundreds of nanometers. As the mode spacing increases, however, the influence of dispersion in the mirror reflection will arise and must be accounted for. Second, by use of an optical reference, we demonstrate that for small (4 μm) excursions of the cavity length, we can lock the lasers to the cavity resonances with an rms uncertainty of 55 Hz. This corresponds to a limiting absolute uncertainty of 2.3 nm rms in inferring the cavity length using the rf method. We will soon introduce a frequency comb locked to an atomic clock to provide a better optical standard. We expect that the ultimate limitation on the measurement accuracy will be provided by uncertainty in the laser lock point about the cavity resonances and should lead to sub-picometer accuracy over our full target range of 50 mm.

References

[1] Arden W 2006 Future semiconductor material requirements and innovations as projected in the ITRS 2005 roadmap *Mater. Sci. Eng.* B **134** 104–8

[2] Bobroff N 1993 Recent advances in displacement measuring interferometry *Meas. Sci. Technol.* **4** 907–26

[3] Pisani M 2008 Multiple reflection Michelson interferometer with picometer resolution *Opt. Express* **16** 21558–63

[4] Pisani M 2009 A homodyne Michelson interferometer with sub-picometer resolution *Meas. Sci. Technol.* **20** 084008

[5] Kren P and Balling P 2009 Common path two-wavelength homodyne counting interferometer development *Meas. Sci. Technol.* **20** 084009

[6] Howard L, Stone J and Fu J 2001 Real-time displacement measurements with Fabry–Perot cavity and a diode laser *Precis. Eng.* **25** 321–35

[7] Joo K-N, Ellis J D, Spronck J W and Munnig Schmidt R H 2009 Design of a folded, multi-pass Fabry–Perot cavity for displacement metrology *Meas. Sci. Technol.* **20** 107001

[8] Hoogenboom B W *et al* 2005 A Fabry–Perot interferometer for micrometer-sized cantilevers *Appl. Phys. Lett.* **86** 074101

[9] Smith D T, Pratt J R and Howard L P 2009 A fiber-optic interferometer with subpicometer resolution for dc and low-frequency displacement measurement *Rev. Sci. Instrum.* **80** 035105

[10] Lawall J 2005 Fabry–Perot metrology for displacements up to 50 mm *J. Opt. Soc. Am.* A **22** 2786–98

[11] Schibli T R, Minoshima K, Bitou Y, Hong F-L, Inaba H, Onae A and Matsumoto H 2006 Displacement metrology with sub-picometer resolution in air based on a fs-comb wavelength synthesizer *Opt. Express* **14** 5984–93

[12] Bitou Y 2009 Displacement metrology directly linked to a time standard using an optical-frequency-comb generator *Opt. Lett.* **34** 1540–2

[13] Clothier W K 1964 A calculable standard of capacitance *Metrologia* **1** 36–55

[14] Durand M, Lawall J and Wang Y 2010 Fabry–Perot displacement interferometry for next-generation calculable capacitor *Conf. on Precision Electromagnetic Measurements (13–18 June 2010)* doi:10.1109/CPEM.2010.5544283 pp 111–2

[15] Cundiff S T and Ye J 2003 Colloquium: femtosecond optical frequency combs *Rev. Mod. Phys.* **75** 325–42